

MALAYSIAN JOURNAL OF ANALYTICAL SCIENCES



Journal homepage: https://mjas.analis.com.my/

Research Article

Phenolic and chlorogenic acid recovery from *Solanum lasiocarpum* Dunal (terung asam) via solid-phase extraction: Fractionation, antioxidant, molecular docking, and anti-obesity

Aniza Saini¹, Mohammad Amil Zulhilmi Benjamin², Muhammad Daniel Eazzat Mohd Rosdan¹, Mohamad Norisham Mohamad Rosdi^{1,3}, Mohd Azrie Awang^{1,4*}

Received: 8 February 2025; Revised: 19 April 2025; Accepted: 23 April 2025; Published: 29 June 2025

Abstract

Solanum lasiocarpum Dunal, commonly known as 'terung asam,' is a fruit-vegetable extensively cultivated on Borneo Island. This study aimed to fractionate chlorogenic acid (CGA) from *S. lasiocarpum* fruit crude extract (SLFCE) using solid-phase extraction and to evaluate its antioxidant and anti-obesity properties. Various ethanol concentrations were tested to determine the fraction yield (FY), total phenolic content (TPC), and CGA content. Antioxidant capacity was assessed using DPPH, ABTS, and FRAP assays. Anti-obesity potential was investigated through *in silico* molecular docking and *in vitro* pancreatic lipase inhibition assays. The 80% ethanol fraction exhibited the highest FY (81.10 ± 0.50%), TPC (34.47 ± 1.41 mg GAE/g), and CGA concentration (7.09 ± 0.27 mg/g). Antioxidant activity was also greatest at this concentration, with DPPH scavenging activity at 91.32 ± 0.61%, ABTS at 85.98 ± 0.09%, and FRAP at 819.53 ± 0.30 mg TE/g. Molecular docking analysis showed that CGA had a stronger binding affinity (–8.3 kcal/mol) than orlistat (–7.6 kcal/mol). *In vitro*, SLFCE and its optimal fraction demonstrated IC₅₀ values of 44.12 ± 0.08 μg/mL and 16.54 ± 0.05 μg/mL, respectively, while CGA and orlistat exhibited IC₅₀ values of 8.45 ± 0.03 μg/mL and 12.71 ± 0.03 μg/mL. These results suggest that SLCFE has promising potential as a functional food ingredient and dietary supplement with notable antioxidant and anti-obesity effects.

Keywords: Solanum lasiocarpum, chlorogenic acid, solid-phase extraction, antioxidant, anti-obesity

Introduction

Among physical methods, solid-phase extraction (SPE) is a highly regarded technique for fractionating complex mixtures, particularly in analytical chemistry and biochemistry. It simplifies the processes of separation, purification, and concentration of bioactive substances, making it valuable for applications in pharmaceuticals, biological samples, natural compounds, pesticides, environmental pollutants, and food and beverages. SPE serves as an efficient alternative to liquid–liquid extraction by addressing issues such as excessive organic solvent usage, lengthy procedures, multiple steps, risk of errors, and high costs [1]. Its ability to separate

components with varying polarity makes it especially effective for processing complex matrices such as plant extracts.

Solanum lasiocarpum Dunal, native to the tropical regions of Southeast Asia, particularly Sarawak, Malaysia, and commonly known as 'terung asam', is a prominent member of the Solanaceae family. It is highly valued for its culinary use as a flavouring agent and its potential as a functional food, being rich in nutrients such as vitamins, minerals, and antioxidant phytochemicals [2]. Soon and Ding [3] examined ethnobotanical records that highlight its use in India for treating fever, vomiting, sore throat, gonorrhoea,

¹ Faculty of Food Science and Nutrition, Universiti Malaysia Sabah, Jalan UMS, 88400, Kota Kinabalu, Sabah, Malaysia

² Borneo Research on Algesia, Inflammation and Neurodegeneration (BRAIN) Group, Faculty of Medicine and Health Sciences, Universiti Malaysia Sabah, Jalan UMS, 88400, Kota Kinabalu, Sabah, Malaysia

³ Nutrition in Community Engagement (NICE) Living Laboratory, Faculty of Food Science and Nutrition, Universiti Malaysia Sabah, Jalan UMS, 88400, Kota Kinabalu, Sabah, Malaysia

⁴ Food Security Research Laboratory, Faculty of Food Science and Nutrition, Universiti Malaysia Sabah, Jalan UMS, 88400, Kota Kinabalu, Sabah, Malaysia

^{*}Corresponding author: ma.awang@ums.edu.my

and female reproductive disorders. The berries and roots are noted for their anti-tussive, anti-asthmatic, anti-rheumatic. anti-viral. anti-cancer. spermicidal properties. However, research on the medicinal applications of this plant remains scarce. Chlorogenic acid (CGA), as shown in Figure 1, is a major polyphenolic compound widely recognised for its health benefits. It is commonly found in various plant sources, particularly green coffee beans, and its structure is formed through the conjugation of the hydroxyl group of quinic acid with the carboxyl group of caffeic acid [4,5]. CGA exhibits a wide range of biological activities, including neuroprotection in neurodegenerative disorders and diabetic neuropathy, well as anti-inflammatory, antioxidant, antimicrobial, and anti-tumour effects. It also mitigates cardiovascular and skin diseases, diabetes, and liver and kidney injuries, primarily by regulating inflammation, oxidative stress, and metabolic homeostasis [5].

Despite significant advancements in extraction techniques, isolating bioactive compounds such as CGA from complex plant matrices remains challenging, particularly for underutilised plants like S. lasiocarpum. The limited understanding of efficient fractionation-based extraction methods and their impact on compound yields and bioactivity underscores the need for systematic investigation. This study aims to optimise the recovery of fraction yield (FY), total phenolic content (TPC), and CGA from S. lasiocarpum fruit crude extract (SLFCE) using SPE, while evaluating its antioxidant and antiobesity properties. By leveraging efficient and sustainable extraction techniques, this research seeks to establish an optimised method for CGA isolation and explore its potential as a functional food and dietary supplement.

Materials and Methods Chemicals and reagents

NADES consisting of choline chloride and lactic acid, together with methanol, ethanol, acetonitrile, and acetic acid (all obtained from Merck, Darmstadt, Germany), were employed as solvents for the extraction process. Sigma-Aldrich (Burlington, MA, USA) provided ascorbic acid (AA), aluminium chloride, potassium dichromate, 2,2-diphenyl-1-picrylhydrazyl (DPPH) reagent, Folin–Ciocalteu (F–C) reagent, sodium carbonate, gallic acid, 2,2-azino-bis(3-ethylbenzothiazoline-6-sulfonic acid) (ABTS) reagent, potassium persulfate, Trolox, acetate buffer,

2,4,6-tripyridyl-s-triazine (TPTZ), hydrochloric acid (HCl), ferric chloride, dimethyl sulfoxide (DMSO), porcine pancreatic lipase, and p-nitrophenyl butyrate (PNPB).

Plant materials

S. lasiocarpum fruits were purchased from a vendor at a local market in Sarawak, washed with distilled water to remove dirt and impurities, arranged on aluminium trays, and dried in an oven (ED 23, Binder, Neckarsulm, Germany) at 50 °C for 140 min. The dried fruits were then ground into a fine powder (< 2 mm).

Preparation of crude extract

The dried and ground fruit of *S. lasiocarpum* (5 g) was extracted in 148.40 mL of natural deep eutectic solvent (NADES), composed of choline chloride and lactic acid, with a solid-to-solvent ratio of 1:29.68 g/mL. The mixture underwent ultrasound-assisted extraction using an ultrasonic probe (Q500 Sonicator, QSonica, Newtown, CT, USA) operating at 57% amplitude for 8.93 min. The solid residues were then filtered using filter paper. To concentrate the crude extract yield, the excess NADES solution was removed using a rotary evaporator (Laborota 4000, Heidolph, Schwabach, Germany) at 50 °C. Finally, the SLFCE was dried in an oven at 50 °C for 24 h.

Fractionation using solid-phase extraction

SPE was performed according to the protocol by Awang et al. [6] with slight modifications, where the dried SLFCE was reconstituted in ethanol (1 mL). The solution was loaded onto a prepared and activated reversed-phase cartridge, Chromabond (Macherey-Nagel, Düren, Germany), with a specification of 45 µm, 6 mL/500 mg, to fractionate the SLFCE into individual fractions (FR-SLFCE). The cartridge was activated by sequential elution with 10 mL of deionised water followed by 10 mL of ethanol. The activated cartridge was then connected to an SPE vacuum manifold system. Fractionation was conducted by gradually eluting the SLFCE solution with an eluent system (0%, 20%, 40%, 60%, 80%, and 100% v/v ethanol concentrations) into collection tubes at a controlled flow rate under a constant pressure of 20 kPa. The compound-saturated eluent collected from the cartridge outlet was dried, and its FY was determined and calculated based on Equation (1).

$$FY (\%) = \frac{\text{Mass of collected fraction (g)}}{\text{Mass of loaded SLFCE (g)}} \times 100$$
 (1)

Malays. J. Anal. Sci. Volume 29 Number 3 (2025): 1460

Figure 1. Chemical structure of CGA.

Total phenolic content

The method used to determine the TPC of FR-SLFCE was adapted from Mohd Rosdan et al. [7] with some modifications, employing the F-C method. Approximately 0.5 mL of FR-SLCFE was mixed with 0.5 mL of 10% F-C reagent. After 3 min, 1.5 mL of 20% sodium carbonate was added to the mixture. The mixture was then kept in the dark at room temperature for 2 h. Absorbance was measured at 765 nm using an ultraviolet-visible (UV-Vis) spectrophotometer (Lambda 25, PerkinElmer, Waltham, MA, USA). Gallic acid was used as the standard reference for constructing the calibration curve. Results were expressed as mg GAE per g of extract, as shown in Equation (2).

TPC (mg GAE/g) =
$$\frac{c \times V}{m}$$
 (2)

where c represents the concentration of FR-SLCFE (mg/mL) obtained from the standard curve of TPC, V represents the sample volume (mL), and m represents the sample mass (mg).

Chlorogenic acid quantification

The quantitative analysis of CGA was performed using high-performance liquid chromatography, adapted from a previous study by Ivanović et al. [8] with slight modifications. A Waters system (Milford, MA, USA), consisting of a binary pump, system controller (Model 2690), automatic sampler, and photodiode array detector (Model 966) was employed for chromatographic separation. The analysis was conducted using a C18 reversed-phase column (Phenomenex, Torrance, CA, USA) with a particle size of 5 μ m and dimensions of 250 × 4.6 mm. The mobile phase consisted of acetonitrile (mobile phase A) and acetic acid (mobile phase B), delivered via isocratic elution. The flow rate was maintained at $0.80\,\text{mL/min}$, with an injection volume of $20\,\mu\text{L}$. CGA was detected at 325 nm, and the column temperature was set at 30 °C. The CGA content was calculated using Equation (3).

$$CGA (mg/g) = \frac{Mass of CGA (mg)}{Dried mass of FR-SLFCE (g)}$$
(3)

Antioxidant assays

The DPPH inhibition activity was estimated using the method of Awang et al. [9] with minor modifications. A 1 mL aliquot of 1 mg/mL FR-SLFCE was mixed with 1 mL of 0.1 mM DPPH solution and incubated in the dark at room temperature for 30 min. Absorbance was measured at 517 nm using a UV-Vis spectrophotometer. A blank DPPH solution served as the negative control, while AA was used as the positive control. The DPPH inhibition activity was calculated using Equation (4).

DPPH inhibition activity (%) =
$$\frac{A_c - A_s}{A_c} \times 100$$
 (4)

where A_c represents the absorbance of the control, and A_s represents the absorbance of the sample.

The ABTS inhibition activity was determined according to the method of Wołosiak et al. [10] with slight modifications. Equal volumes of ABTS solution (7 mM) and potassium persulfate (2.45 mM) were mixed, and the reaction was carried out in the dark at room temperature for 12 h. The resulting ABTS solution was diluted with acetate buffer at pH 3.6, and its absorbance was adjusted to 0.70 ± 0.02 at 734 nm using a microplate reader (Multiskan SkyHigh, Thermo Fisher Scientific, Waltham, MA, USA). A 20 μL aliquot of 1 mg/mL FR-SLFCE was then mixed with 120 μL of the ABTS solution. The reaction was allowed to proceed for 6 min, after which the absorbance was measured again at 734 nm. A blank ABTS solution served as the negative control, while Trolox was used as the positive control. The ABTS inhibition activity was calculated using Equation (5).

ABTS inhibition activity (%) =
$$\frac{A_c - A_s}{A_c} \times 100$$
 (5)

where A_c represents the absorbance of the control, and A_s represents the absorbance of the sample.

The ferric reducing antioxidant power (FRAP) assay was conducted as described by Russo et al. [11] with slight modifications. The FRAP reagent was freshly prepared before each measurement by mixing acetate

buffer (300 mM), TPTZ solution (10 mM in 40 mM HCl), and ferric chloride (20 mM) in a ratio of 10:1:1 (v/v/v), followed by incubation at 37 °C for up to 30 min. For the analysis, 180 μ L of FRAP reagent was mixed with 20 μ L of FR–SLFCE and incubated for 10 min at 37 °C before measuring the absorbance at 593 nm. Trolox was used as the standard antioxidant to generate a calibration curve based on linear regression, as calculated in Equation (6).

FRAP (mg TE/g) =
$$\frac{c \times V}{m}$$
 (6)

where c represents the concentration of FR-SLFCE (mg/mL) obtained from the standard curve of FRAP, V represents the sample volume (mL), and m represents the sample mass (mg).

In silico molecular docking

Molecular docking was performed following the method of Li et al. [12] with some alterations. In this study, CGA was selected as the target ligand (Table 1), while orlistat served as the reference ligand. The 3D molecular structures of the ligands were retrieved from PubChem and converted to .pdb format using BIOVIA Discovery Studio Visualiser software (Version 4.5). Pancreatic lipase (PDB ID: 1ETH) was used as the binding target, and its 3D structure was obtained from the **RCSB** (https://www.rcsb.org/). Docking between the ligands and the protein was conducted using the CB-Dock2 web server (https://cadd.labshare.cn/cb-dock2/). CB-Dock2 predicts protein binding sites and determines their centres and sizes using a curvature-based cavity detection approach. The server is integrated with AutoDock Vina software (Version 1.2.4) and is optimised to achieve over 70% success in model prediction. The analysis was performed using protein files in .pdb format and ligands in .sdf format, with five potential binding cavities identified. The cavity with the lowest binding energy was selected based on the Vina score. The best binding conformation was further evaluated for molecular interactions with receptor residues using the same software. Validation was performed by comparing the docking structure of pancreatic lipase (1ETH) with its co-crystallised ligands, hydroxyethyloxytri(ethyloxy)octane (C8E) and CGA.

Table 1. Characteristics of ligands used in docking analysis

| | Ligand | PubChem ID |
|-----------|----------|---------------|
| Target | CGA | 1794427 |
| Reference | Orlistat | 3034010 |

In vitro anti-lipase assay

The enzymatic inhibition assay for anti-lipase activity was adopted from Estribillo et al. [13] with minor adaptations. The optimal FR-SLFCE (1 mg) was dissolved in 10 mL of 100 mM phosphate buffer containing 0.5% Triton X-100 at pH 7.2 to prepare a 100 μg/mL stock solution. From this, working solutions at concentrations of 20, 40, 60, 80, and 100 µg/mL were prepared. Orlistat, used as the positive control, was prepared in DMSO. The assay began by adding 25 µL of FR-SLFCE or orlistat to 50 μL of pancreatic lipase solution and mixing gently. This was followed by the addition of 100 µL of buffer solution and 25 µL of PNPB (substrate), and the mixture was mixed gently. The blank was prepared by replacing FR-SLFCE or orlistat with 100 mM phosphate buffer. The reaction mixture was then incubated for 30 min at 37 °C. Pancreatic lipase activity was determined by measuring the hydrolysis of PNPB to p-nitrophenol at 400 nm using a microplate reader. The percentage of pancreatic lipase inhibition was calculated using Equation (7).

Lipase inhibition activity (%) =
$$\frac{A_c - A_s}{A_c} \times 100$$
 (7)

where A_c represents the absorbance of the control, and A_s represents the absorbance of the sample. The results were expressed as IC₅₀ values (half-maximal inhibitory concentration), obtained through regression analysis, representing the concentration required to achieve 50% inhibition of lipase activity.

Statistical analysis

Data were presented as mean \pm standard deviation (SD), based on triplicate measurements. Statistical significance was assessed using one-way ANOVA, followed by Tukey's Honestly Significant Difference (HSD) test at a 95% confidence level (p < 0.05), conducted using GraphPad Prism software (Version 10).

Results and Discussion

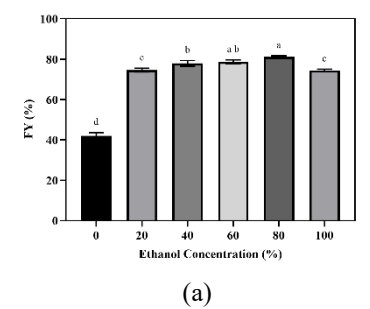
Effect of ethanol concentration on FR-SLFCE of FY, TPC, and CGA

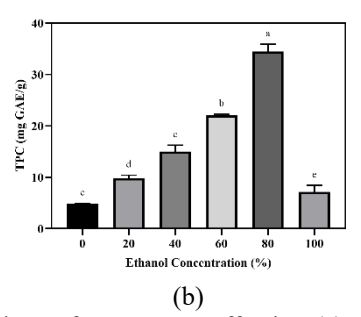
Figures 2(a), 2(b), and 2(c) illustrate the influence of ethanol concentration on FY, TPC, and CGA content in FR-SLFCE. Initially, SLFCE was analysed using yielding HLPC, $1.89 \,\mathrm{mg/g}$ of CGA. chromatograms of CGA, SLFCE, and optimal FR-SLFCE are shown in **Figure 3**. As depicted in **Figure 2(a)**, FY significantly (p < 0.05) increased with rising ethanol concentrations from 0% to 100%, with the highest FY observed at 80% ethanol ($81.10 \pm 0.50\%$), followed by 60% $(78.67 \pm 0.96\%)$ and 40% $(77.90 \pm 1.39\%)$ ethanol. No significant differences were noted at 20% $(74.56 \pm 0.92\%)$ and 100% $(74.43 \pm 0.55\%)$ ethanol (p > 0.05), while the lowest

FY was recorded at 0% ethanol (41.99 \pm 1.63%). Figure 2(b) shows that TPC increased from 0% to 80% ethanol, with the highest value at 80% ethanol $(34.47 \pm 1.41 \text{ mg} \text{ GAE/g})$, followed by 60% $(22.09 \pm 0.19 \text{ mg} \text{ GAE/g}), 40\% (15.00 \pm 1.22 \text{ mg})$ GAE/g), and 20% (9.82 \pm 0.56 mg GAE/g) ethanol. A decline was observed at 100% ethanol (7.13 \pm 1.27 mg GAE/g), likely due to degradation, while the lowest TPC occurred at 0% ethanol $(4.84 \pm 0.09 \text{ mg GAE/g})$. Figure 2(c) further shows that CGA content significantly (p < 0.05) increased with ethanol concentration, peaking at 80% ethanol (7.09 $\pm 0.27 \text{ mg/g}$), followed by 60% (5.22 $\pm 0.08 \text{ mg/g}$) and 40% (5.11 ± 0.12 mg/g) ethanol, with no significant difference between the latter two (p > 0.05). This was followed by 20% ethanol $(2.87 \pm 0.05 \text{ mg/g})$, while the lowest CGA content was recorded at 0% ethanol $(0.64 \pm 0.01 \text{ mg/g})$. A slight decline was also noted at 100% ethanol $(0.79 \pm 0.10 \,\mathrm{mg/g})$. Overall, CGA content in the optimal FR-SLFCE increased substantially from 1.89 mg/g in SLFCE to 7.09 mg/g at 80% ethanol, indicating effective enrichment.

The eluent composition influences van der Waals interactions between the sorbent and compounds present in the crude extract [6], thereby affecting the quality of the resulting fractions as different compounds are selectively recovered. Increasing ethanol concentration reduces the polarity of the eluent system, enabling the elution of relatively non-

polar to semi-polar compounds from the SPE cartridge. Ethanol, particularly at concentrations between 50% and 95%, is widely recognised as an effective solvent for extracting phenolic compounds due to its ability to solubilise both polar and non-polar constituents, thus enhancing the recovery of bioactive compounds [14]. Mixtures of ethanol and water (e.g., 75–80% ethanol) have been shown to produce higher TPC values by more effectively solubilising a broader spectrum of phenolic compounds compared to 100% ethanol [15,16]. This is supported by findings from El Mannoubi [17], who reported the highest yield using 80% ethanol in the extraction of Opuntia stricta fruit. Likewise, a study on honeysuckle reported a sharp increase in CGA content when ethanol concentration was raised from 50% to 70%, followed by a decline beyond this point [18]. An increase in ethanol concentration enhances mass transfer dynamics, improving solvent penetration and CGA dissolution. However, excessively high ethanol concentrations may reduce CGA solubility and increase the presence of alcohol-soluble impurities, ultimately leading to a decline in yield. Supporting this, Oziembłowski et al. [19] demonstrated that 68% ethanol was more effective than 95% ethanol for CGA extraction from elderberry flowers and reduced extraction time from 30 to 20 days. It can be hypothesised that the reduced yield observed at 100% ethanol may be attributed to either the depletion of extractable compounds in the raw material or their increased retention on the adsorbent surface [20].





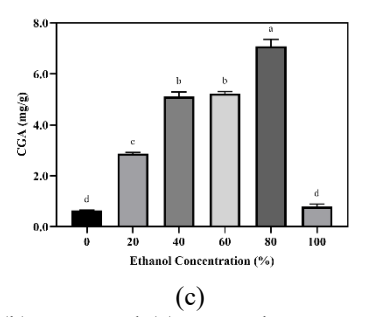


Figure 2. Different ethanol concentrations of FR–SLFCE affecting (a) FY, (b) TPC, and (c) CGA eluents. Data are presented as mean \pm SD (n = 3). Different letters indicate significant differences (p < 0.05) based on one-way ANOVA followed by Tukey's HSD test

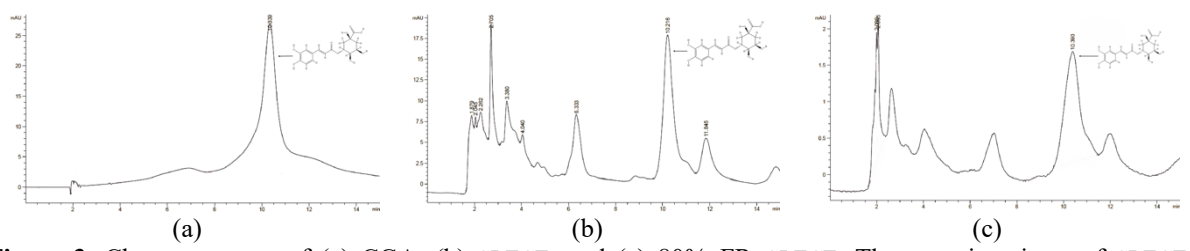


Figure 3. Chromatograms of (a) CGA, (b) SLFCE, and (c) 80%–FR–SLFCE. The retention times of SLFCE (10.300 min) and FR–SLFCE (10.390 min) were compared with that of CGA (10.339 min), showing a high degree of similarity

Effect of ethanol concentration of FR-SLFCE on antioxidant activity

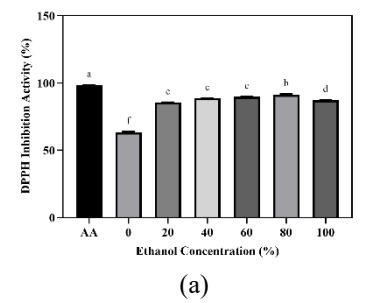
The DPPH inhibition activity of FR-SLFCE is shown in Figure 4(a), with AA used as the positive control. The results indicated that the 80% ethanol exhibited the highest inhibition $(91.32 \pm 0.61\%)$ with significant differences (p < 0.05),followed 60% $(89.76 \pm 0.25\%)$, 40% $(88.69 \pm 0.21\%)$, and 20% $(87.21 \pm 0.39\%)$ ethanol, among which no significant differences were found (p > 0.05). This was followed by 100% ethanol ($85.68 \pm 0.13\%$), while the lowest inhibition was recorded at 0% ethanol $(63.38 \pm 0.59\%)$. Similarly, the ABTS inhibition activity of FR-SLFCE is presented in Figure 4(b), with Trolox used as the positive control. The 80% the ethanol showed highest inhibition $(85.98 \pm 0.09\%)$, followed by 60% $(85.66 \pm 0.09\%)$ and 40% ($85.53 \pm 0.04\%$) ethanol, which differed slightly but significantly (p < 0.05). This was followed by 100% (85.42 \pm 0.04%) and 20% (85.39 \pm 0.04%) ethanol, between which no significant differences were observed (p > 0.05). The lowest ABTS inhibition was seen at 0% ethanol (85.12 \pm 0.09%).

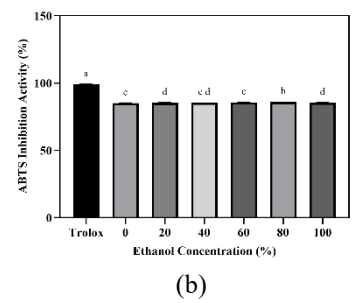
Additionally, the FRAP activity of FR–SLFCE is presented in **Figure 4(c)**. The highest activity was recorded at 80% ethanol (819.53 \pm 0.30 mg TE/g), showing a significant difference (p < 0.05) compared to 100% (791.48 \pm 5.39 mg TE/g) and 60% (633.67 \pm 8.12 mg TE/g) ethanol. Meanwhile, 40% (570.05 \pm 0.59 mg TE/g) and 20% (557.14 \pm 0.15 mg TE/g) ethanol did not differ significantly (p > 0.05). The lowest FRAP activity was observed at 0% ethanol (174.14 \pm 9.93 mg TE/g).

The highest antioxidant activity was observed at 80% ethanol concentration for DPPH, ABTS, and FRAP, indicating that FR–SLFCE contains higher antioxidant compounds when extracted with 80% ethanol as the eluent. Research demonstrates that 80% ethanol effectively elutes compounds due to its

moderate polarity, which reduces the co-elution of unwanted substances. A previous study supports these findings, showing that stevia leaf extracts exhibited higher antioxidant properties, particularly in DPPH and ABTS inhibition, when using 80% ethanol [21]. Similarly, a study on Nephelium mutabile rind reported that among ethanol concentrations (40%, 60%, and 80%), 80% ethanol yielded the highest DPPH inhibition and FRAP activity [22]. Phenolic compounds in SLFCE dissolve effectively in aqueous ethanol under optimal conditions. Polar solvents efficiently extract phenolic compounds by disrupting hydrogen bonds within polyphenol structures, thereby enhancing their solubility in organic solvents [23]. Additionally, ethanol disrupts cell walls by weakening hydrogen bonds and dissolving lipid membranes, thus facilitating the release of intracellular metabolites, including polyphenols, which contribute antioxidant activity.

CGA often shows a stronger correlation in DPPH assays compared to ABTS and FRAP. The chemical structure and antioxidant mechanism of CGA make it more compatible with the DPPH assay. CGA reacts rapidly with DPPH radicals, leading to a quick and measurable change in absorbance, which enhances the sensitivity and accuracy of the DPPH assay. Research indicates a high correlation between DPPH and TPC in various plant extracts, suggesting that phenolic compounds like CGA are effectively measured by DPPH assays [24]. While the ABTS assay is also based on radical scavenging, it involves a different radical (ABTS) and may not be as sensitive to the specific type of antioxidant activity exhibited by CGA [25]. The FRAP assay measures the reducing power of antioxidants by assessing their ability to reduce Fe³⁺ to Fe²⁺ [26]. The antioxidant activity of CGA is more related to hydrogen atom donation, making it less directly comparable to the focus of the FRAP assay on electron transfer.





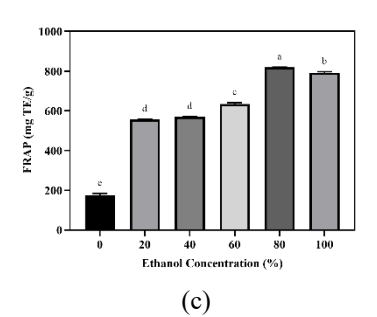


Figure 4. Different ethanol concentrations of FR–SLFCE affecting (a) DPPH, (b) ABTS, and (c) FRAP for antioxidant activity. Data are presented as mean \pm SD (n = 3). Different letters indicate significant differences (p < 0.05) based on one-way ANOVA followed by Tukey's HSD test

In silico molecular docking of pancreatic lipase

Table 2 presents the binding affinity of CGA against the pancreatic lipase receptor, with orlistat as the reference ligand. Since binding affinity reflects the inhibitory properties of selected inhibitors, the results indicate that CGA exhibits better binding affinity to pancreatic lipase than orlistat. The docked CGA yielded a Vina score of -8.3 kcal/mol, demonstrating its ability to interact with pancreatic lipase with higher affinity compared to orlistat, which yielded a Vina score of -7.6 kcal/mol. A negative Vina score indicates that the interaction between the ligand and the target protein requires minimal energy to occur, signifying a thermodynamically favourable binding process [27]. This result suggests a strong affinity between the two molecules, as lower binding energy generally corresponds to more stable and effective molecular interactions.

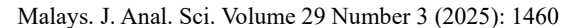
The docked pose of CGA formed interactions through five hydrogen bonds, one π – π T-shaped interaction, and two π – π stacked interactions (**Figure 5**). Molecular docking studies have demonstrated that ligands can exhibit significant binding interactions through various non-covalent forces, including π – π interactions. For instance, in a study involving the docking of compounds to a receptor, strong π – π interactions with specific amino acid residues were shown to enhance binding affinities [28]. These findings highlight the importance of such interactions when evaluating the potential of new drug candidates. In this study, CGA formed interactions with His264, Ser154, and Asp80, with hydrogen bond distances of

3.54 Å, 2.35 Å, and 2.54 Å, respectively. Similarly, orlistat interacted with His264 and Asp80, forming a hydrogen bond at 4.25 Å and an electrostatic interaction at 4.24 Å, respectively (**Figure 6**). The binding of CGA to pancreatic lipase likely involves multiple amino acid residues within the active site of the enzyme. Key residues such as Ser153, Asp177, and His264, which form the catalytic triad essential for lipase activity, are believed to contribute to enhanced binding affinities for both CGA and orlistat [29,30].

The amino acids that occupy the same binding pore in both the co-crystallised protein and the CGA compound are Asp80, Ile79, His152, Phe78, and Val260, with a binding affinity of −3.2 kcal/mol. This indicates that Asp80, Ile79, His152, Phe78, and Val260 are in the same positions (binding sites) in both the protein structure (with the original co-crystallised ligand) and the CGA compound. These amino acids are part of the protein active site or binding region where interaction with the ligand (in this case, the CGA compound) occurs. If the CGA compound fits into the protein binding site in a manner like the original co-crystallised ligand, it suggests that the binding mechanism is comparable [31]. This implies that docking validation was successful. Binding affinity reflects how strongly the compound (CGA) binds to the protein. The lower (more negative) the value, the stronger the binding interaction [32]. A value of -8.3 kcal/mol suggests that the binding between the CGA compound and the lipase protein is reasonably strong.

Table 2. Docking results for CGA and orlistat: Vina scores, interactions, and bond distances

| Ligand | Vina Score (kcal/mol) | Interacting | Types of Bonds | Distance (Å) |
|----------|-----------------------|-------------|----------------------|--------------|
| | | Amino Acid | | |
| CGA | -8.3 | Arg257 | Conventional | 2.04 |
| | | Asp80 | hydrogen bond | 2.54 |
| | | Ser154 | | 2.35 |
| | | His152 | Carbon hydrogen bond | 3.46 |
| | | His264 | | 3.54 |
| | | Phe78 | π–π T-Shaped | 3.93 |
| | | Tyr115 | π–π Stacked | 5.04 |
| | | Phe216 | | 5.18 |
| Orlistat | -7.6 | Phe78 | Conventional | 5.44 |
| | | His152 | hydrogen bond | 4.22 |
| | | Gly77 | | 3.29 |
| | | Asp80 | Attractive charge | 4.24 |
| | | His264 | Carbon hydrogen bond | 4.25 |
| | | Ala216 | Alkyl | 4.92 |
| | | Ile79 | | 4.65 |
| | | Pro181 | | 5.90 |
| | | Phe216 | π–Alkyl | 6.30 |
| | | | | 4.55 |
| | | Tyr115 | | 4.77 |
| | | | | 4.36 |



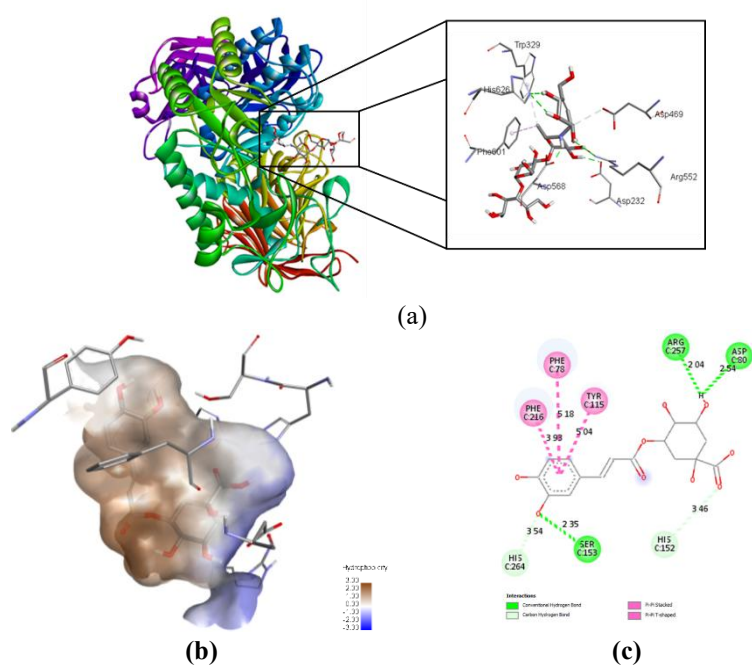


Figure 5. Visualisation of CGA docking interaction with pancreatic lipase: (a) 3D representation of the interaction between CGA and amino acid residues; (b) 3D representation of the hydrophobicity surface; (c) 2D representation illustrating CGA binding to the active site of pancreatic lipase

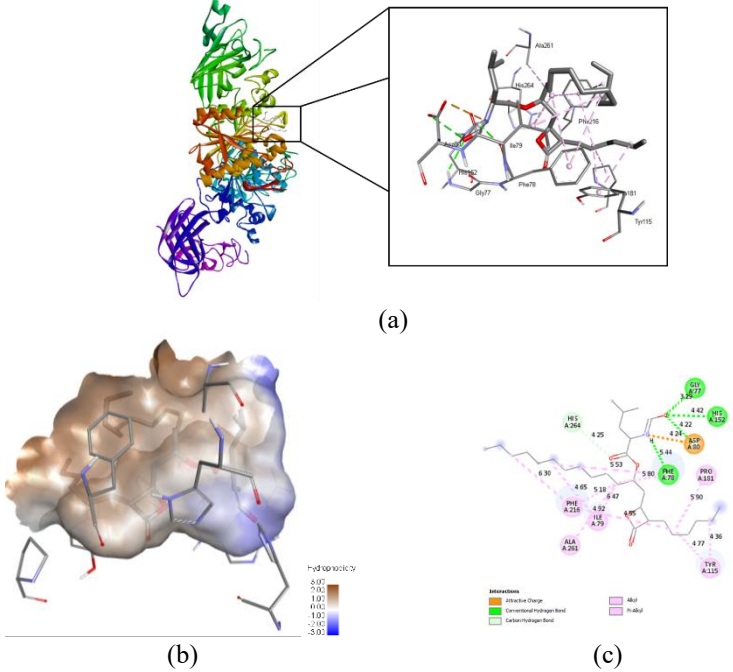
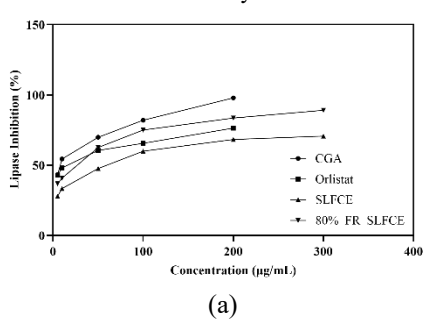


Figure 6. Visualisation of orlistat docking interaction with pancreatic lipase: (a) 3D representation of the interaction between orlistat and amino acid residues; (b) 3D representation of the hydrophobicity surface; (c) 2D representation illustrating orlistat binding to the active site of pancreatic lipase



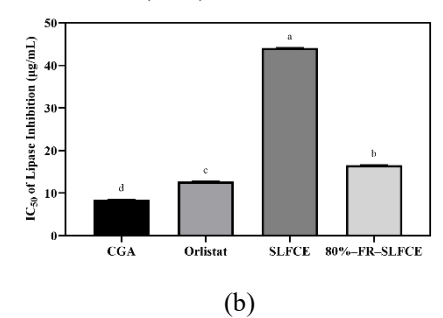


Figure 7. Pancreatic lipase inhibitory activity of CGA, orlistat, SLFCE, and 80%–FR–SLFCE. (a) Inhibition at different concentrations; (b) IC₅₀ values of inhibition. Data are presented as mean \pm SD (n = 3). Different letters indicate significant differences (p < 0.05) based on one-way ANOVA followed by Tukey's HSD test

In vitro anti-lipase activity of pancreatic lipase

Figure 7 compares the lipase inhibitory activity of CGA, orlistat, SLFCE, and 80%-FR-SLFCE against pancreatic lipase. The results indicate that standard CGA exhibited the lowest IC₅₀ value (8.45 \pm 0.031 μg/mL), signifying the highest inhibitory activity, followed by orlistat (IC₅₀ = $12.71 \pm 0.03 \mu g/mL$). The 80%-FR-SLCFE showed greater inhibitory activity, with an IC₅₀ of $16.54 \pm 0.05 \mu g/mL$, compared to SLFCE (IC₅₀ = $44.12 \pm 0.02 \, \mu g/mL$), reflecting the increased purity of CGA in the FR-SLFCE. Research demonstrates that CGA inhibits pancreatic lipase through a mixed-type inhibitory mechanism, allowing binding to both the free enzyme and the enzymesubstrate complex with varying affinities [33], as evidenced by in silico molecular docking, which revealed interactions between CGA and key residues such as His264, Asp177, and Ser153 within the catalytic triad essential for lipase function. Additionally, the presence of phenolic compounds in SLFCE may contribute to the overall inhibitory effect, as phenolics inhibit pancreatic lipase by targeting core pathways, including PI3K-Akt, MAPK, prolactin, and cAMP signalling pathways, highlighting potential therapeutic targets for obesity management [34]. Furthermore, fractionation enhances bioactivity by isolating more potent compounds, as observed in 80%-FR-SLFCE, thereby increasing efficacy in lipase inhibition. Supporting this, a study on the ethyl acetate fraction of Cynometra cauliflora leaves found it to be an active lipase inhibitor with strong bioactivity [35].

Conclusion

This study demonstrates the efficacy of SPE using 80% ethanol in optimising the fractionation of FY (81.10 \pm 0.50%), TPC (34.47 \pm 1.41 mg GAE/g), and CGA (7.09 \pm 0.27 mg/g) from SLFCE. The resulting extract also exhibited high antioxidant potential, as indicated by DPPH (91.32 \pm 0.61%), ABTS (85.98 \pm 0.09%), and FRAP (819.53 \pm 0.30 mg TE/g) values. *In silico* molecular docking revealed that CGA shows promising activity in inhibiting pancreatic lipase,

comparable to orlistat. In vitro, the IC50 of 80%–FR–SLFCE (16.54 \pm 0.05 $\mu g/mL)$ demonstrated potent activity, slightly lower than CGA (8.45 \pm 0.031 $\mu g/mL)$ and orlistat (12.71 \pm 0.03 $\mu g/mL), but significantly stronger than SLFCE (44.12 <math display="inline">\pm$ 0.02 $\mu g/mL)$. These findings indicate that 80%–FR–SLFCE serves as a rich source of phenolic compounds, particularly CGA, with strong antioxidant and anti-obesity potential, highlighting the suitability of this extract as a valuable ingredient for functional foods and dietary supplements.

Acknowledgement

The authors express their sincere appreciation to the Faculty of Food Science and Nutrition, Universiti Malaysia Sabah, for providing the necessary facilities and financial support. This research was funded by Universiti Malaysia Sabah through the Geran Bantuan Penyelidikan Pascasiswazah (UMSGreat) [Grant Number GUG0678-1/2024].

References

- 1. Badawy, M. E. I., El-Nouby, M. A. M., Kimani, P. K., Lim, L. W. and Rabea, E. I. (2022). A review of the modern principles and applications of solid-phase extraction techniques in chromatographic analysis. *Analytical Sciences*, 38 (12): 1457-1487.
- 2. Hui-Yan, T. and Sarbini, S. R. (2024). The local indigenous food of Sarawak as potential functional food. *International Journal of Food Science & Technology*, 59(10): 7692-7703.
- 3. Soon, A. T. K. and Ding, P. (2021). A review on wild indigenous eggplant, terung asam Sarawak (*Solanum lasiocarpum* Dunal.). *Sains Malaysiana*, 50 (3): 595-603.
- Pimpley, V., Patil, S., Srinivasan, K., Desai, N. and Murthy, P. S. (2020). The chemistry of chlorogenic acid from green coffee and its role in attenuation of obesity and diabetes. *Preparative Biochemistry and Biotechnology*, 50 (10): 969-978.

- Nguyen, V., Taine, E. G., Meng, D., Cui, T. and Tan, W. (2024). Chlorogenic acid: A systematic review on the biological functions, mechanistic actions, and therapeutic potentials. *Nutrients*, 16 (7): 924.
- Awang, M. A., Chua, L. S. and Abdullah, L. C. (2022). Solid-phase extraction and characterization of quercetrin-rich fraction from *Melastoma malabathricum* leaves. *Separations*, 9(11): 373.
- 7. Mohd Rosdan, M. D. E., Awang, M. A., Benjamin, M. A. Z., Mohd Amin, S. F. and Julmohammad, N. (2024). Effect of ultrasound-assisted osmotic dehydration (UAOD) pretreatment on *Mangifera pajang* Kosterm. fruit pulp: Drying kinetics, chemical qualities, and color measurement. *Journal of Food Process Engineering*, 47(9): e14721.
- 8. Ivanović, M., Grujić, D., Cerar, J., Razboršek, M. I., Topalić-Trivunović, L., Savić, A., Kočar, D. and Kolar, M. (2022). Extraction of bioactive metabolites from *Achillea millefolium* L. with choline chloride based natural deep eutectic solvents: A study of the antioxidant and antimicrobial activity. *Antioxidants*, 11(4): 724.
- Awang, M. A., Benjamin, M. A. Z., Anuar, A., Ismail, M. F., Ramaiya, S. D. and Mohd Hashim, S. N. A. (2023). Dataset of gallic acid quantification and their antioxidant and antiinflammatory activities of different solvent extractions from kacip fatimah (*Labisia pumila* Benth. & Hook. f.) leaves. *Data in Brief*, 51: 109644.
- Wołosiak, R., Drużyńska, B., Derewiaka, D., Piecyk, M., Majewska, E., Ciecierska, M., Worobiej, E. and Pakosz, P. (2022). Verification of the conditions for determination of antioxidant activity by ABTS and DPPH assays—a practical approach. *Molecules*, 27(1): 50.
- Russo, D., Kenny, O., Smyth, T. J., Milella, L., Hossain, M. B., Diop, M. S., Rai, D. K. and Brunton, N. P. (2013). Profiling of phytochemicals in tissues from *Sclerocarya* birrea by HPLC-MS and their link with antioxidant activity. ISRN Chromatography, 2013: 283462.
- 12. Li, S., Pan, J., Hu, X., Zhang, Y., Gong, D. and Zhang, G. (2020). Kaempferol inhibits the activity of pancreatic lipase and its synergistic effect with orlistat. *Journal of Functional Foods*, 72: 104041.
- 13. Estribillo, A. G. M., Gaban, P. J. V., Rivadeneira, J. P., Villanueva, J. C., Torio, M. A. O. and Castillo-Israel, K. A. T. (2022). Evaluation of in vitro lipid-lowering properties of 'Saba' banana [Musa acuminata x balbisiana (BBB group) 'Saba'] peel pectin from different extraction

- methods. *Malaysian Journal of Nutrition*, 28(1): 65-77.
- 14. Dirar, A. I., Alsaadi, D. H. M., Wada, M., Mohamed, M. A., Watanabe, T. and Devkota, H. P. (2019). Effects of extraction solvents on total phenolic and flavonoid contents and biological activities of extracts from Sudanese medicinal plants. South African Journal of Botany, 120: 261-267.
- Sun, C., Wu, Z., Wang, Z. and Zhang, H. (2015). Effect of ethanol/water solvents on phenolic profiles and antioxidant properties of Beijing propolis extracts. *Evidence-Based Complementary and Alternative Medicine*, 2015: 595393.
- Yusof, N., Abdul Munaim, M. S. and Veloo Kutty, R. (2020). The effects of different ethanol concentration on total phenolic and total flavonoid content in Malaysian Propolis. *IOP Conference Series: Materials Science and Engineering*, 991(1): 012033.
- 17. El Mannoubi, I. (2023). Impact of different solvents on extraction yield, phenolic composition, *in vitro* antioxidant and antibacterial activities of deseeded *Opuntia stricta* fruit. *Journal of Umm Al-Qura University for Applied Sciences*, 9 (2): 176-184.
- Cui, T., Wang, C., Shan, C. and Wu, P. (2014).
 Optimization of the extraction technology of chlorogenic acid in honeysuckle response surface method. *Open Access Library Journal*, 1 (6): e941.
- Oziembłowski, M., Nawirska-Olszańska, A. and Maksimowski, D. (2023). Optimization of chlorogenic acid in ethanol extracts from elderberry flowers (Sambucus nigra L.) under different conditions: Response surface methodology. Applied Sciences, 13(5): 3201.
- 20. Osorio, E., Toledano, M., Aguilera, F. S., Tay, F. R. and Osorio, R. (2010). Ethanol wet-bonding technique sensitivity assessed by AFM. *Journal of Dental Research*, 89 (11): 1264-1269.
- Chakma, A., Afrin, F., Rasul, M. G., Maeda, H., Yuan, C. and Shah, A. K. M. A. (2023). Effects of extraction techniques on antioxidant and antibacterial activity of stevia (Stevia rebaudiana Bertoni) leaf extracts. Food Chemistry Advances, 3: 100494.
- Sopee, M. S. M., Azlan, A. and Khoo, H. E. (2019). Comparison of antioxidants content and activity of Nephelium mutabile rind extracted using ethanol and water. Journal of Food Measurement and Characterization, 13(3): 1958-1963.
- 23. Sun, S., Liu, Z., Lin, M., Gao, N. and Wang, X. (2024). Polyphenols in health and food processing: Antibacterial, anti-inflammatory,

- and antioxidant insights. Frontiers in Nutrition, 11: 1456730.
- 24. Clarke, G., Ting, K. N., Wiart, C. and Fry, J. (2013). High correlation of 2,2-diphenyl-1-picrylhydrazyl (DPPH) radical scavenging, ferric reducing activity potential and total phenolics content indicates redundancy in use of all three assays to screen for antioxidant activity of extracts of plants from the Malaysian rainforest. *Antioxidants*, 2 (1): 1-10.
- Sadeer, N. B., Montesano, D., Albrizio, S., Zengin, G. and Mahomoodally, M. F. (2020). The versatility of antioxidant assays in food science and safety—chemistry, applications, strengths, and limitations. *Antioxidants*, 9(8): 709
- 26. Hsieh, C. and Rajashekaraiah, V. (2021). Ferric reducing ability of plasma: A potential oxidative stress marker in stored plasma. *Acta Haematologica Polonica*, 52(1): 61-67.
- Macari, G., Toti, D., Pasquadibisceglie, A. and Polticelli, F. (2020). DockingApp RF: A state-ofthe-art novel scoring function for molecular docking in a user-friendly interface to AutoDock Vina. *International Journal of Molecular* Sciences, 21(24): 9548.
- Shao, J., Kuiper, B. P., Thunnissen, A.-M. W. H., Cool, R. H., Zhou, L., Huang, C., Dijkstra, B. W. and Broos, J. (2022). The role of tryptophan in π interactions in proteins: An experimental approach. *Journal of the American Chemical Society*, 144 (30): 13815-13822.
- Zhu, Y.-T., Jia, Y.-W., Liu, Y.-M., Liang, J., Ding, L.-S. and Liao, X. (2014). Lipase ligands in Nelumbo nucifera leaves and study of their binding mechanism. Journal of Agricultural and Food Chemistry, 62(44): 10679-10686.

- 30. Mudgil, P., Baba, W. N., Kamal, H., FitzGerald, R. J., Hassan, H. M., Ayoub, M. A., Gan, C.-Y. and Maqsood, S. (2022). A comparative investigation into novel cholesterol esterase and pancreatic lipase inhibitory peptides from cow and camel casein hydrolysates generated upon enzymatic hydrolysis and in-vitro digestion. *Food Chemistry*, 367: 130661.
- Du, X., Li, Y., Xia, Y.-L., Ai, S.-M., Liang, J., Sang, P., Ji, X.-L. and Liu, S.-Q. (2016). Insights into protein-ligand interactions: Mechanisms, models, and methods. *International Journal of Molecular Sciences*, 17(2): 144.
- 32. Quek, A., Kassim, N. K., Lim, P. C., Tan, D. C., Mohammad Latif, M. A., Ismail, A., Shaari, K. and Awang, K. (2021). α-Amylase and dipeptidyl peptidase-4 (DPP-4) inhibitory effects of *Melicope latifolia* bark extracts and identification of bioactive constituents using *in vitro* and *in silico* approaches. *Pharmaceutical Biology*, 59(1): 964-973.
- 33. Xu, Z., Cao, Q., Manyande, A., Xiong, S. and Du, H. (2022). Analysis of the binding selectivity and inhibiting mechanism of chlorogenic acid isomers and their interaction with grass carp endogenous lipase using multi-spectroscopic, inhibition kinetics and modeling methods. *Food Chemistry*, 382: 132106.
- 34. Liu, Y., Luo, J. and Xu, B. (2024). Elucidation of anti-obesity mechanisms of phenolics in *Artemisiae argyi* Folium (Aiye) by integrating LC-MS, network pharmacology, and molecular docking. *Life*, 14(6): 656.
- 35. Ado, M. A., Abas, F., Mohammed, A. S. and Ghazali, H. M. (2013). Anti- and pro-lipase activity of selected medicinal, herbal and aquatic plants, and structure elucidation of an anti-lipase compound. *Molecules*, 18(12): 14651-14669.